


# Non–Small-Cell Lung Cancer: Feasibility of Intratumoral Radiofrequency Hyperthermia–enhanced Herpes Simplex Virus Thymidine Kinase Gene Therapy

Jiansong Ji, MD, PhD • Qiaoyou Weng, MS • Feng Zhang, MD, PhD • Fu Xiong, MD, PhD • Yin Jin, MD • Junguo Hui, MD • Jingjing Song, MD • Jun Gao, MD, PhD • Minjiang Chen, MS • Qiang Li, MD, PhD • David Shin, MD • Xiaoming Yang, MD, PhD

From the Image-Guided Bio-Molecular Interventions Research and Division of Interventional Radiology, Department of Radiology, University of Washington School of Medicine, 850 Republican St, S470, Seattle, WA 98109 (J.J., Q.W., F.Z., F.X., Y.J., J.S., J.G., M.C., Q.L., D.S., X.Y.); Key Laboratory of Imaging Diagnosis and Minimally Invasive Interventional Research of Zhejiang Province, Department of Radiology, Zhejiang University Lishui Hospital, Lishui, Zhejiang, China (J.J., Q.W., J.H., J.S., M.C., Q.L.); and Sir Run Run Shaw Hospital, Zhejiang University School of Medicine, Hangzhou, Zhejiang, China (Y.J., X.Y.). Received August 7, 2017; revision requested November 20, 2017; accepted February 6, 2018. **Address correspondence** to X.Y. (e-mail: [xmyang@uw.edu](mailto:xmyang@uw.edu)).

Supported by Natural Science Funding of Zhejiang Province (LQ16H160019), Social Applied Research Plan Programs of Science and Technology Commission of Zhejiang Province of China (2016C37100), Key Program of National Natural Science Foundation of China (81430040), and the National Institutes of Health (R01EBO12467), and Key Program of Zhejiang Province (2018C03024).

Conflicts of interest are listed at the end of this article.

Radiology 2018; 288: 612–620 • <https://doi.org/10.1148/radiol.2018172148> • Content code: 

**Purpose:** To validate the feasibility and efficacy of intratumoral radiofrequency hyperthermia (RFH)-enhanced herpes simplex virus (HSV) thymidine kinase (TK) and ganciclovir (GCV) (hereafter, HSV-TK/GCV) gene therapy for non–small-cell lung cancer (NSCLC).

**Materials and Methods:** This study was performed from November 11, 2015, to April 14, 2017, and included (a) *in vitro* experiments with human NSCLC cells to establish the proof of principle, (b) *in vivo* experiments using mice with subcutaneous NSCLC to further demonstrate the principle, and (c) *in vivo* experiments using rats with orthotopic NSCLC to validate the technical feasibility. Cells, nude mice, and nude rats were randomly divided into four groups (six animals per group): (a) combination therapy (HSV-TK/GCV combined with RFH), (b) RFH, (c) HSV-TK/GCV, and (d) phosphate-buffered saline. Data were analyzed by using the Dunnett *t* test or Kruskal–Wallis test.

**Results:** For *in vitro* experiments, the cell proliferation assay showed significantly diminished viable cells with combination therapy (mean, 0.56; 95% confidence interval [CI]: 0.44, 0.68) versus RFH (mean, 0.89; 95% CI: 0.82, 0.97), HSV-TK/GCV (mean, 0.71; 95% CI: 0.56, 0.86), and phosphate-buffered saline (mean, 1; 95% CI: 1, 1) ( $P < .05$  for all). For *in vivo* experiments, optical imaging showed significantly decreased relative bioluminescence signal with combination therapy (mean, 0.71 [95% CI: 0.03, 1.39] in mice; 1.29 [95% CI: 0.51, 2.06] in rats) compared with RFH (mean, 2.66 [95% CI: 1.73, 3.59] in mice; 2.26 [95% CI: 1.51, 3.01] in rats), HSV-TK/GCV (mean, 1.37 [95% CI: 0.65, 2.08] in mice; 1.76 [95% CI: 1.20, 2.31] in rats), and phosphate-buffered saline (mean, 3.07 [95% CI: 2.50, 3.65] in mice; 2.94 [95% CI: 2.29, 3.58] in rats) ( $P < .001$  for all). US showed that the smallest relative tumor volumes occurred with combination therapy (mean, 0.60; 95% CI: 0.15, 1.05) versus RFH (mean, 2.43; 95% CI: 1.80, 3.06), HSV-TK/GCV (mean, 1.32; 95% CI: 0.75, 1.89), and phosphate-buffered saline (mean, 2.56; 95% CI: 1.75, 3.38) ( $P < .05$  for all) in the mouse subcutaneous model.

**Conclusion:** Intratumoral radiofrequency hyperthermia–enhanced herpes simplex virus thymidine kinase and ganciclovir gene therapy for non–small-cell lung cancer is feasible and can be guided by molecular imaging.

©RSNA, 2018

**N**on–small-cell lung cancer (NSCLC) constitutes about 80% of pulmonary malignant tumors (1). Although surgical resection is the standard of care for early-stage NSCLC (2), most of the patients with lung cancer are not eligible for surgery at the time of diagnosis because of locally advanced disease, poor cardiopulmonary function, or other medical comorbidities (3,4).

During the past decade, imaging-guided percutaneous thermal ablation techniques, such as radiofrequency ablation and microwave ablation, have emerged as minimally invasive, low-cost, and repeatable approaches for local tumor control of unresectable NSCLC (5–7). However, it is challenging to achieve a sufficient and predictable volume of coagulative necrosis within and around the tumor (so-called surgical margin, 10 mm from the tumor edge) because of the

heat-sink effect of the surrounding blood flow in the bronchovascular network and the low conductivity of the aerated lung parenchyma (6,8). In addition, the undertreated lung tumors often recur with infiltrative growth patterns to form microsatellite lesions or microvenous tumor emboli (6).

Suicide gene therapy is a promising method with which to treat cancer. One of the most commonly recognized suicide gene therapy systems uses the thymidine kinase (TK) gene of the herpes simplex virus (HSV). The TK gene expressed in cancer cells can phosphorylate a prodrug, ganciclovir (GCV), into the active triphosphate form, which kills not only the targeted tumor cells but also neighboring cells via the bystander effect (9). HSV-TK and GCV–mediated suicide gene therapy (hereafter, HSV-TK/GCV) has been investigated as an effective and valuable approach in

## Abbreviations

CI = confidence interval, GCV = ganciclovir, GFP = green fluorescent protein, HSV = herpes simplex virus, NSCLC = non-small-cell lung cancer, RFH = radiofrequency hyperthermia, SI = signal intensity, TK = thymidine kinase, TUNEL = terminal deoxynucleotidyl transferase-mediated 2'-deoxyuridine, 5'-triphosphate nick end labeling

## Summary

Radiofrequency hyperthermia-enhanced gene therapy may introduce a paradigm for effective management of unresectable lung cancer by integrating the advantages of interventional molecular imaging with direct intratumoral gene therapy.

## Implication for Patient Care

This technical development may introduce a paradigm for effective management of unresectable lung cancer by integrating the advantages of interventional molecular imaging, radiofrequency technology, and direct intratumoral gene therapy.

the treatment of many cancer types, such as hepatocellular carcinoma (10), ovarian cancer (11), and NSCLC (12). Although the efficacy of HSV-TK/GCV has been confirmed in studies of cancer cells and rodent models, it has not been demonstrated in clinical studies, primarily because of the low gene transduction efficiency via systemic administration (13). Direct intratumoral injection of high-dose HSV-TK genes using radiofrequency hyperthermia (RFH) is a proposed solution to improve the HSV-TK gene transfection and thus maximize its clinical potential (14–16). The aim of our study was to validate the feasibility of implementing intratumoral RFH-enhanced HSV-TK/GCV gene therapy for NSCLC by using molecular imaging.

## Materials and Methods

### Study Design

The institutional animal care and use committee approved the animal protocols. This single-center study was divided into three phases: (a) *in vitro* evaluation to establish proof of principle for RFH-enhanced HSV-TK/GCV gene therapy in human NSCLC cells, (b) *in vivo* confirmation of the concept in mouse models with subcutaneous NSCLC xenografts, and (c) *in vivo* validation of the technical feasibility of molecular imaging-monitored intratumoral RFH-enhanced HSV-TK/GCV gene therapy in rat models with orthotopic NSCLC (Fig 1).

### In Vitro Evaluation

**Experimental set-up.**—Human NSCLC cells (A549, ATCC, Manassas, Va) were transfected with mCherry/luciferase lentiviral particles to create mCherry/luciferase-positive cells according to the manufacturer's protocol (GeneCopoeia, Rockville, Md). Recombinant green fluorescent protein (GFP)/HSV-TK lentiviral particles were produced by transient transfection of 293FT cells with GFP/HSV-TK lentiviral plasmid vectors and third-generation lenti-combo packing mix, according to the manufacturer's protocol (Applied Biologic Materials, Richmond, British Columbia, Canada) (17). Because GFP and HSV-TK gene expressions were simultaneously driven by the

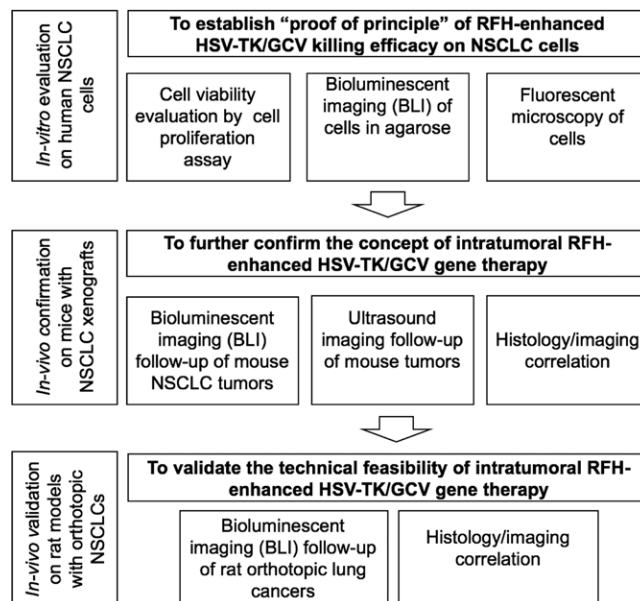


**Figure 1:** Flowchart shows study design and implementation. *In vitro* experiments using human non-small-cell lung cancer (NSCLC) cells (A549) labeled with mCherry/luciferase/lentivirus, *in vivo* experiments in mice with subcutaneous lung cancers, and *in vivo* experiment in rats with orthotopic human lung cancers were divided into four treatment groups: (a) combination therapy (herpes simplex virus [HSV] thymidine kinase [TK]/ganciclovir [GCV] gene therapy combined with radiofrequency hyperthermia [RFH]), (b) RFH alone, (c) HSV-TK/GCV gene therapy, and (d) phosphate-buffered saline.

same promoter, the detection of GFP with optical imaging allowed for the assessment of HSV-TK expression.

A total of  $2 \times 10^4$  A549 mCherry/luciferase-positive cells were seeded in a 24-well cell culture plate (Becton Dickinson, Franklin Lakes, NJ). Cells were collected at 1, 2, 3, 5, and 7 days after the GFP/HSV-TK lentiviral infection for quantitative analysis of GFP expression with flow cytometry and GFP fluorescence microscopy.

**RFH-enhanced gene therapy.**—A total of  $2.5 \times 10^4$  luciferase-positive A549 cells were seeded in four-chamber cell culture slides that were placed in a 37°C water bath (NalgeNunc International, Rochester, NY). The cells were treated with (a) combination therapy of GFP/HSV-TK plus RFH at 41°C–42°C for 30 minutes and subsequent GCV exposure (hereafter, combination therapy), (b) RFH alone, (c) GFP/HSV-TK gene therapy alone, and (d) phosphate-buffered saline. RFH was performed by attaching a custom-made 0.022-inch radiofrequency heating wire under the bottom of the chamber and connecting it to a radiofrequency generator. A sterilized 1.1-mm fiberoptic temperature probe was placed in the bottom of each chamber and connected to a thermometer (PhotonControl, Burnaby, British Columbia, Canada) for real-time monitoring of the temperatures during the RFH.

Cell viability was evaluated via a cell proliferation assay 72 hours after GCV treatment. The absorbance was measured at 490 nm (SpectraMax; Molecular Devices, Sunnyvale, Calif). Relative cell proliferations were evaluated by using the following

equation:  $(A_{\text{treated}} - A_{\text{blank}})/(A_{\text{control}} - A_{\text{blank}})$ , where  $A_{\text{treated}}$  is the absorbance of the treated cells,  $A_{\text{blank}}$  is absorbance of cell culture medium, and  $A_{\text{control}}$  is the absorbance of cells in the control group. Cells on slides were subsequently counterstained with 4',6-diamidino-2-phenylindole (Vector Laboratories, Burlingame, Calif) and were imaged with fluorescent microscopy. The experiment was repeated six times in each group.

In vitro bioluminescent imaging was performed for the other set of four treatment groups. Cells in each group were treated with 5  $\mu\text{L}$  of Pierce d-Luciferin (ThermoFisher Scientific, Rockford, Ill). Then, 50  $\mu\text{L}$  of cells were mixed with 50  $\mu\text{L}$  of 1% agarose (Invitrogen, Carlsbad, Calif) in a transparent cylindrical glass tube for optical imaging (In-Vivo Xtreme; Bruker, Billerica, Mass). Bioluminescent signal intensity was calculated as the mean of all detected photon counts within a manually derived region of interest by using MI software (Bruker). Relative signal intensity ( $SI_{\text{relative}}$ ) was determined with the following equation:  $SI_{\text{relative}} = SI_{\text{treatment}}/SI_{\text{control}}$ , where  $SI_{\text{treatment}}$  represents signal intensity in the treatment group and  $SI_{\text{control}}$  represents signal intensity in the control group.

### In Vivo Confirmation in Mice with NSCLC Xenografts

#### Creation of mouse models with NSCLC xenografts.—

Treatments were performed in nude mice (Charles River Laboratories, Wilmington, Mass) with subcutaneous NSCLC xenografts, created by inoculating  $(0.5\text{--}1.0) \times 10^7$  A549 mCherry/luciferase cells into the subcutaneous tissue of the back unilaterally. Once the tumor reached 5–8 mm in diameter, we started treatment procedures.

#### RFH-enhanced HSV-TK gene therapy of mouse tumors.—

Twenty-four female mice with subcutaneous tumors were randomly allocated to four treatment groups (six animals per group): (a) combination therapy with 50  $\mu\text{L}$  GFP/HSV-TK gene therapy with RFH at 41°C–42°C for 30 minutes, followed by 7 days of intraperitoneal injection of 5 mg per kilogram of body weight GCV, (b) RFH alone, (c) HSV-TK/GCV gene therapy alone, and (d) phosphate-buffered saline. With US guidance (Sonosite, Bothell, Wash), the custom-made 0.022-inch RF heating guidewire was inserted into the tumor, with its hot spot at the center of each mass, while a 400- $\mu\text{m}$  microfiber optical thermal probe was placed at the tumor margin for instant measurement of temperature within the radiofrequency-heated tumor.

US was performed to measure tumor size changes at 0, 7, and 14 days after treatment. Tumor size was measured in three orthogonal axes, with the x- and y-axes defining the largest planar dimension and the z-axis defining the depth. The volume ( $V$ ) of each tumor was calculated with the following equation:  $V = x \times y \times z \times \pi/6$ , where  $x$ ,  $y$ , and  $z$  refer to the axes. Data were normalized to relative tumor volume ( $V_{\text{relative}}$ ) by using the following equation:  $V_{\text{relative}} = V_{\text{Dn}}/V_{\text{D0}}$ , where  $V_{\text{Dn}}$  represents volume at a given number of days after treatment, and  $V_{\text{D0}}$  represents volume the day before treatment.

Bioluminescence imaging was used to acquire the bioluminescence signals of tumors 0, 7, and 14 days after treatment. After intraperitoneal injection of 150 mg/kg of d-luciferin, images were captured at an exposure time of 8 minutes

and an emission wavelength of 530 nm. Signal intensity was quantified by using the aforementioned software. Relative signal intensity ( $SI_{\text{relative}}$ ) was calculated with the equation  $SI_{\text{relative}} = SI_{\text{Dn}}/SI_{\text{D0}}$ , where  $SI_{\text{Dn}}$  stands for signal intensity at a given number of days after treatment and  $SI_{\text{D0}}$  represents signal intensity the day before treatment.

### In Vivo Technical Validation in Rat Models with Orthotopic NSCLC and Clinical Radiofrequency System

#### Creation of rat models with molecular imaging–detectable orthotopic NSCLC.—

Female athymic nude rats (Charles River Laboratories) aged 10–12 weeks were imaged by using an in vivo optical imaging system (In Vivo Xtreme; Bruker). With the x-ray and optical imaging guidance of this imaging system, a 26-gauge needle was percutaneously advanced into the lower lobe of the right lung through the seventh intercostal space at the midaxillary line. A total of  $(0.5\text{--}1.0) \times 10^7$  mCherry/luciferase A549 cells mixed in 20  $\mu\text{L}$  of phosphate-buffered saline, 10  $\mu\text{L}$  of x-ray contrast agent (350 mg iodine per milliliter, Omnipaque; GE Healthcare, Westborough, Mass), and 20  $\mu\text{L}$  of Matrigel (Corning, Bedford, Mass) were injected into the lung parenchyma. The success of intrapulmonary cell inoculation was confirmed by deposition of the x-ray contrast agent in the lung. Bioluminescent imaging was then used to monitor tumor growth every week. When the tumor size reached 8–10 mm, the rat was enrolled for the following treatment.

#### RFH-enhanced HSV-TK gene therapy of orthotopic rat lung tumors.—

Twenty-four female nude rats with orthotopic lung tumors were allocated into four treatment groups: (a) combination therapy of GFP/HSV-TK followed by RFH at 41°C–42°C for 30 minutes followed by 7 days of intraperitoneal injection of 5 mg/kg GCV, (b) RFH alone, (c) HSV-TK/GCV gene therapy alone, and (d) phosphate-buffered saline. A total of 50  $\mu\text{L}$  HSV-TK/lentivirus ( $1 \times 10^8$  plaque-forming units) was directly injected into the tumor via the perfusion needle of an 18-G single polar radiofrequency electrode (Welfaremedic, Beijing, China) under x-ray and optical imaging guidance. The radiofrequency electrode had multiple functions for simultaneously generating radiofrequency heat, therapeutic drug delivery, and temperature monitoring. Immediately after intratumoral gene delivery, RFH at 41°C–42°C was generated, while the temperature in the tumor was monitored with the thermal sensors at the perfusion needle tip of the same electrode. GCV (50 mg/kg) was intraperitoneally administered for 7 days immediately after gene delivery. Bioluminescence imaging was used to follow-up the changes of the bioluminescence signals and sizes of tumors at 7 and 14 days after treatment.

### Immunoblotting

Cells and tumor tissues of the mouse and rat models were processed via homogenization. Proteins (range, 40–80  $\mu\text{g}$ ) were subjected to Western blotting analysis according to the

manufacturer protocol (ThermoFisher Scientific). The level of gene expression was quantified by measuring the density of the immunoreactive bands and subsequently normalizing them to the relative area (RA) according to the following equation:  $RA = A_{\text{RFH+gene}} / A_{\text{gene}}$ , where  $A_{\text{RFH+gene}}$  and  $A_{\text{gene}}$  represent the chemiluminescence area of the RFH+gene and gene, respectively.

### Pathologic Assessment

Tumor tissue samples were fixed in 4% paraformaldehyde solution, embedded in paraffin, and sliced at 5- $\mu\text{m}$  intervals. The tissue slices were stained with hematoxylin-eosin to confirm the formation of cancer nodules. Apoptosis of treated tumors was analyzed with immunohistochemical staining by using the terminal deoxynucleotidyl transferase-mediated 2'-deoxyuridine, 5'-triphosphate nick end labeling (TUNEL) apoptosis detection kit (R&D Systems, Minneapolis, Minn). Ki-67 antibody (Abcam, Cambridge, Mass) was used to evaluate cell proliferation according to the manufacturer protocol.

### Statistical Analyses

Results are expressed as the mean, with 95% confidence intervals (CIs). Statistical analyses were performed by using SPSS 22.0 software (IBM, Chicago, Ill). Two-tailed  $P < .05$  was considered to indicate a significant difference. The Dunnett  $t$  test was used to estimate the relative viabilities of cells assessed with a cell proliferation assay, relative bioluminescent imaging signals, apoptotic index, and sizes of mouse tumors, as well as bioluminescent imaging signals and Ki67 levels of rat tumors, between the combination group and each of the other groups, respectively. The Kruskal-Wallis test was used to compare the relative bioluminescent imaging of cells and apoptotic index of rat tumors between the combination group and each of other groups, respectively. The Student  $t$  test was used to compare GFP/HSV-TK expression levels in lung cancer cells, mouse subcutaneous lung cancers, and rat orthotopic lung cancers between the group with and the group without radiofrequency hyperthermia enhancement.

## Results

### In Vitro Evaluation of RFH-enhanced HSV-TK Killing Effect on NSCLC Cells

Both confocal microscopy (Fig 2a) and flow cytometry (Fig 2b) showed GFP expression reached its peak on day 3 after gene transduction. Confocal microscopy (Fig 3a) qualitatively showed that fewer cells survived combination therapy than survived the other three treatments. Cell proliferation analysis enabled us to confirm cell viability was lower in the combination therapy group than in any other treatment group, manifesting as significantly decreased relative cell proliferation (mean, 0.56 [95% CI: 0.44, 0.68] vs 0.89 [95% CI: 0.82, 0.97] for RFH; 0.71 [95% CI: 0.56, 0.86] for HSV-TK/GCV; and 1 [95% CI: 1, 1] for phosphate-buffered saline; all  $P < .05$ ) (Fig 3b). In addition, the quantitative analysis of cell bioluminescence signal revealed a significant decrease in relative photon signal intensity in the combination therapy group compared with the other treatment groups (mean, 0.17 [95% CI: 0.01, 0.34] vs

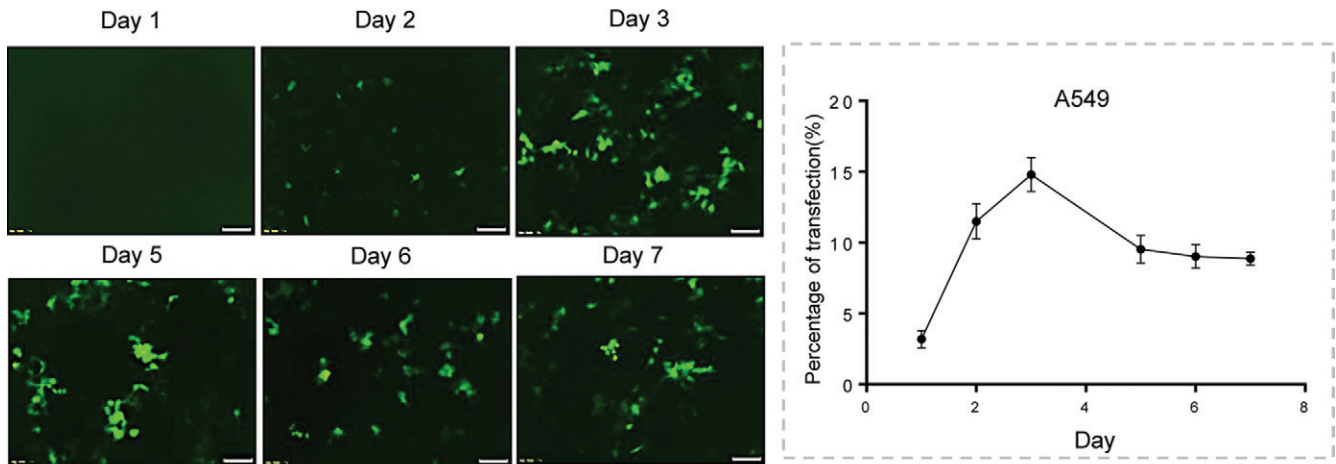
0.85 [95% CI: 0.64, 1.07]; 0.47 [95% CI: 0.10, 0.83], and 1.00 [95% CI: 1.00, 1.00], respectively;  $P < .05$ ) (Fig 3c). Immunoblotting analysis showed that RFH significantly increased GFP/HSV-TK gene expression by 2.11-fold ( $P < .05$ ) compared with no RFH enhancement (Fig 3d).

### In Vivo Confirmation of RFH-enhanced HSV-TK Gene Therapy in Mouse Tumors

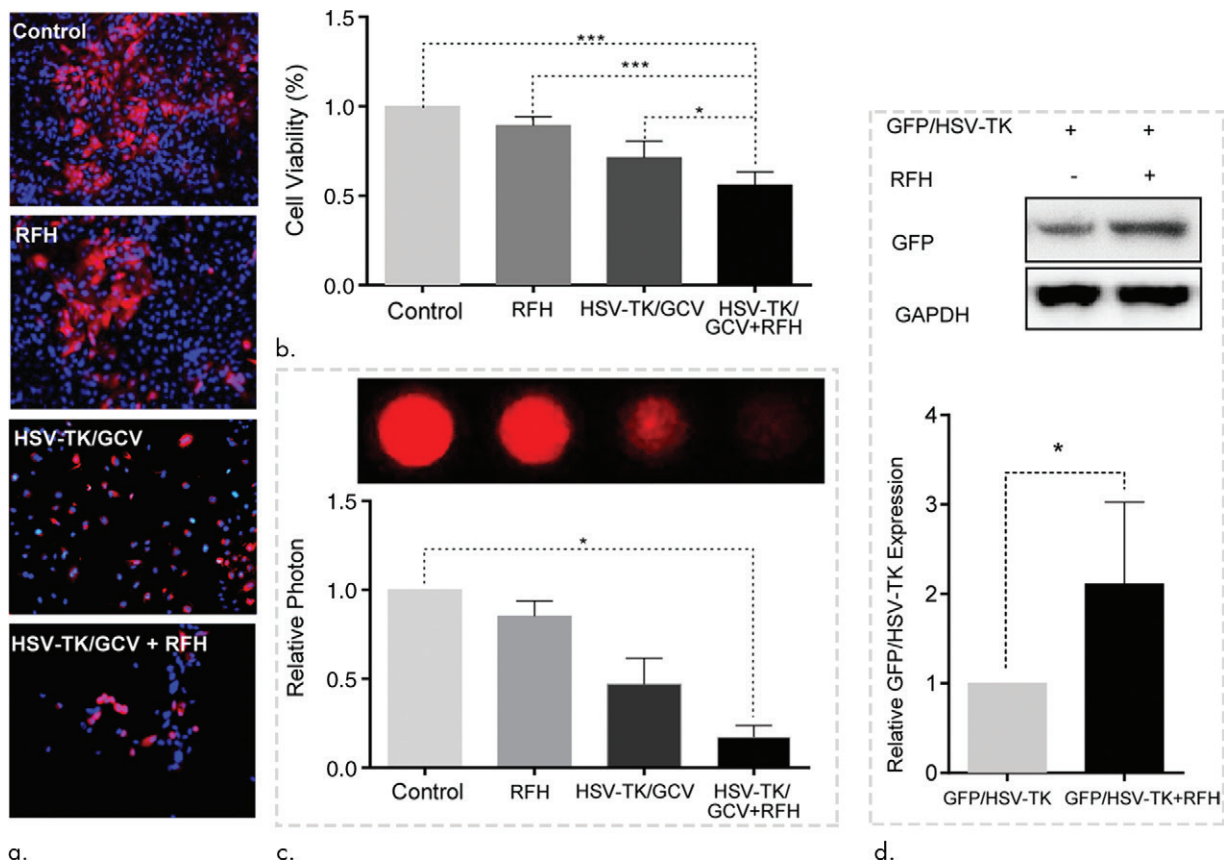
The quantitative analysis of subcutaneous tumor bioluminescence signal in mice showed a significantly reduced bioluminescent signal intensity with combination therapy compared with other treatments (mean, 0.71 [95% CI: 0.03, 1.39] vs 2.66 [95% CI: 1.73, 3.59] for RFH; 1.37 [95% CI: 0.65, 2.08] for HSV-TK/GCV, and 3.07 [95% CI: 2.50, 3.65] for phosphate-buffered saline;  $P < .001$ ) (Fig 4a). US further confirmed that the tumor growth after combination therapy was significantly inhibited, showing as the lowest relative tumor volume compared with other treatments (mean: 0.60 [95% CI: 0.15, 1.05] vs 2.43 [95% CI: 1.80, 3.06] for RFH, 1.32 [95% CI: 0.75, 1.89] for HSV-TK/GCV, and 2.56 [95% CI: 1.75, 3.38] for phosphate-buffered saline; all  $P < .05$ ). Pathologic analysis was correlated with the imaging findings and demonstrated that the smallest tumor size and the highest apoptotic index occurred in the combination therapy group when compared with the other groups (mean: 0.41 [95% CI: 0.36, 0.46] vs 0.04 [95% CI: 0.02, 0.06] for RFH, 0.11 [95% CI: 0.07, 0.14] for HSV-TK/GCV, and 0.01 [95% CI: -0.06, 0.03] for phosphate-buffered saline; all  $P < .001$ ) (Fig 4c). Furthermore, the Western blotting analysis of gene expression in tumor tissues (Fig 4d) displayed a 1.79-fold increase in GFP/HSV-TK gene expression with combination therapy compared with GFP/HSV-TK gene transduction alone ( $P < .01$ ).

### RFH-enhanced Direct Intratumoral HSV-TK Gene Therapy for Rat Orthotopic NSCLC

Bioluminescence imaging analysis and histologic assessment enabled us to confirm the technical feasibility of directly inoculating NSCLC cells in the rat lung to create an orthotopic lung cancer model (Fig 5). Within 2–3 weeks after percutaneous intrapulmonary tumor cell inoculation (Fig 5a, 5b), optical imaging depicted bioluminescence signals emitting from the tumors (Fig 5c). These tumors were confirmed as adenocarcinoma at subsequent pathologic evaluation (Fig 5d). With x-ray and optical imaging guidance, GFP/HSV-TK/lentiviruses were percutaneously injected into the lung tumors by using the perfusion needle of the radiofrequency electrode (Fig 6). Follow-up bioluminescence imaging (Fig 7a, 7b) demonstrated a significantly lower relative photon signal intensity of tumors in the combination therapy group than in the other groups (mean: 1.29 [95% CI: 0.51, 2.06] vs 2.26 [95% CI: 1.51, 3.01] for RFH, 1.76 [95% CI: 1.20, 2.31] for HSV-TK/GCV, and 2.94 [95% CI: 2.29, 3.58] for phosphate-buffered saline;  $P < .001$ ). Gross pathologic evaluation revealed tumor size was smallest in the combination therapy group (Fig 7a). Immunoblotting analysis indicated that intratumoral RFH increased GFP/HSV-TK gene expression by 57% ( $P < .05$ ) (Fig 7c). Immunohistochemical analysis (Fig 8

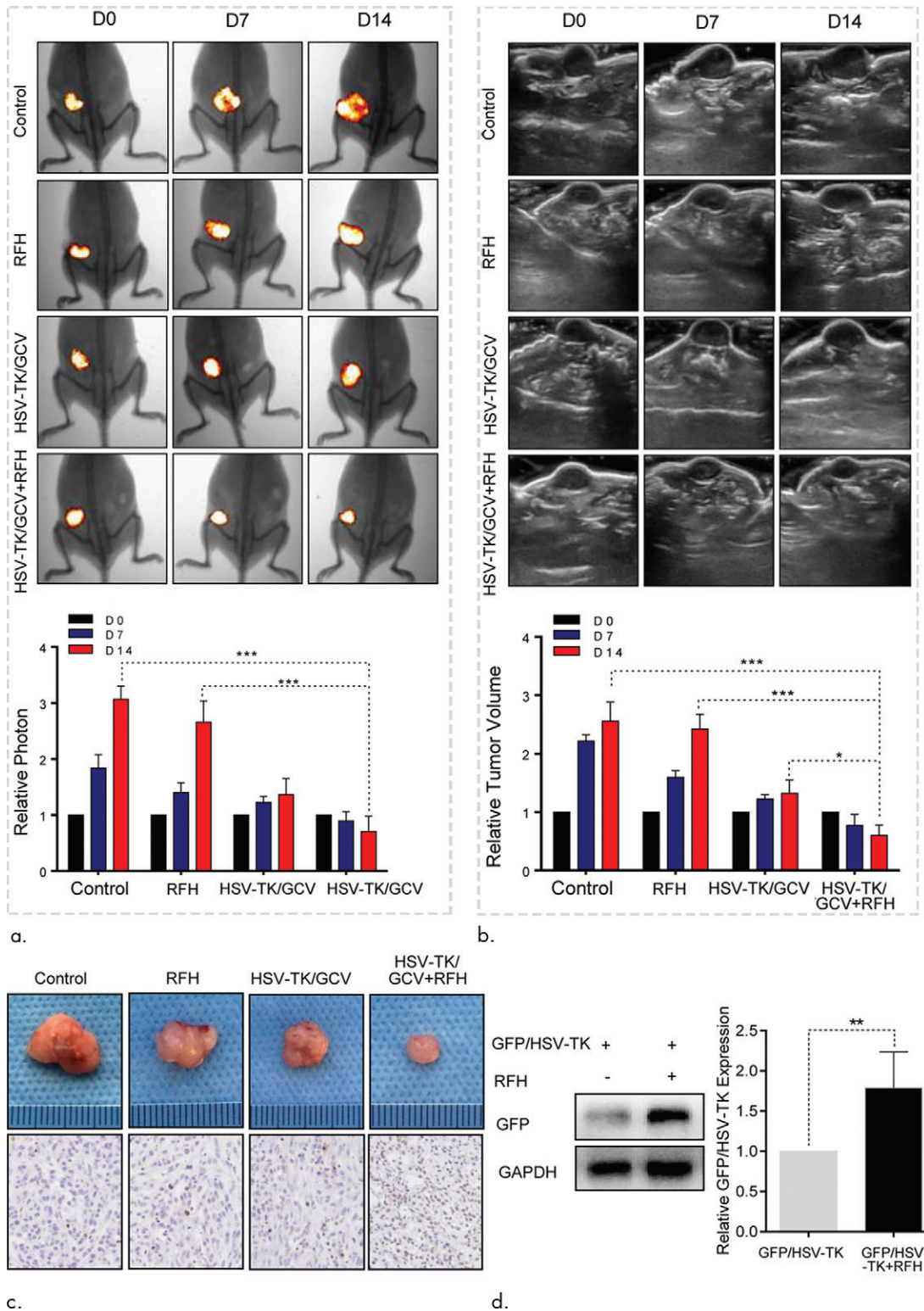


**Figure 2:** Human lung adenocarcinoma cells (A549) were transduced with green fluorescent protein (GFP)/herpes simplex virus thymidine kinase/lentiviral particles. **(a)** Fluorescent microscopy showed increasing expression of GFP in cells over 7 days. **(b)** Quantitative assay with flow cytometry enabled confirmation of the level of GFP gene expression (mean  $\pm$  standard deviation), reaching a peak on day 3 after gene transduction and maintaining a relatively high level over the following days.



**Figure 3:** In vitro experiments on therapeutic effect of different treatments on various cell groups. **(a)** Confocal microscopy showed that fewer cells survived in the combination therapy group than in the other three groups. **(b)** Cell proliferation analysis showed the lowest cell viability in the combination therapy group compared with the other groups (mean: herpes simplex virus [HSV] thymidine kinase [TK]/ganciclovir [GCV] plus radiofrequency hyperthermia [RFH], 0.56 [95% confidence interval {CI}]: 0.44, 0.68] vs radiofrequency hyperthermia [RFH], 0.89 [95% CI: 0.82, 0.97]; HSV-TK/GCV, 0.71 [95% CI: 0.56, 0.86]; and phosphate-buffered saline, 1 [95% CI: 1, 1]; all  $P < .05$ ). Error bar indicates standard deviation of cell viability. **(c)** In vitro quantitative bioluminescence analysis further demonstrated the lowest photon signal in cells treated with combination therapy (mean: HSV-TK/GCV plus RFH, 0.17 [95% CI: 0.01, 0.34] vs RFH, 0.85 [95% CI: 0.64, 1.07]; HSV-TK/GCV, 0.47 [95% CI: 0.10, 0.83]; and phosphate-buffered saline, 1.00 [95% CI: 1.00, 1.00];  $P < .05$ ). Error bar indicates standard deviation of relative photon. **(d)** Western blotting analysis confirmed increased expression of green fluorescent protein (GFP) in cells treated with RFH compared with cells without RFH treatment (mean: GFP/HSV-TK plus RFH, 2.11 [95% CI: 1.15, 3.07] vs GFP/HSV-TK, 1.00 [95% CI: 1.00, 1.00];  $P < .05$ ; six animals per group). Error bar indicates standard deviation of relative gene expression level. GAPDH = glyceraldehyde 3-phosphate dehydrogenase. \* =  $P < .05$ , \*\* =  $P < .01$ , and \*\*\* =  $P < .001$ .

**Figure 4:** In vivo experiments for establishing proof of principle by using nude mice with subcutaneous xenografts of lung tumors. Bioluminescence imaging and US were used to monitor responses of tumors to different treatments over time (herpes simplex virus [HSV] thymidine kinase [TK]/ganciclovir [GCV] plus radiofrequency hyperthermia [RFH], RFH alone, HSV-TK/GCV alone, and phosphate-buffered saline). **(a)** X-ray and optical imaging revealed a significant decrease of mean photon signals (red-yellow) in the combination therapy group (mean: HSV-TK/GCV plus RFH, 0.71 [95% confidence interval (CI): 0.03, 1.39] vs RFH, 2.66 [95% CI: 1.73, 3.59]; HSV-TK/GCV, 1.37 [95% CI: 0.65, 2.08]; and phosphate-buffered saline, 3.07 [95% CI: 2.50, 3.65];  $P < .001$ ). Error bars show the standard deviation. **(b)** US showed that the smallest mean tumor size occurred with combination therapy compared with the other treatments (mean: HSV-TK/GCV plus RFH, 0.60 [95% CI: 0.15, 1.05] vs RFH, 2.43 [95% CI: 1.80, 3.06]; HSV-TK/GCV, 1.32 [95% CI: 0.75, 1.89]; and phosphate-buffered saline, 2.56 [95% CI: 1.75, 3.38]; all  $P < .05$ ). Error bars show the standard deviation. **(c)** Assessment of gross specimens of tumors confirmed that the smallest tumor size occurred in the combination therapy group (upper panel). Terminal deoxynucleotidyl transferase-mediated 2'-deoxyuridine, 5'-triphosphate nick end labeling staining for apoptosis analysis (original magnification,  $\times 200$ ) displayed more apoptotic cells (brown stains, lower panel) in the combination therapy group than in the other groups (mean: HSV-TK/GCV plus RFH, 0.41 [95% CI: 0.36, 0.46] vs RFH, 0.04 [95% CI: 0.02, 0.06]; HSV-TK/GCV, 0.11 [95% CI: 0.07, 0.14]; and phosphate-buffered saline, 0.01 [95% CI: -0.06, 0.03]; all  $P < .001$ ). **(d)** Western blotting analysis confirmed a significant increase of GFP gene expression in tumors treated with RFH compared with tumors without RFH treatment (mean: [green fluorescent protein [GFP]/HSV-TK plus RFH, 1.79 [95% CI: 1.32, 2.26] vs GFP/HSV-TK, 1.00 [95% CI: 1.00, 1.00];  $P < .01$ ;  $n = 6$  per group]. Error bars show the standard deviation. GAPDH = glyceraldehyde 3-phosphate dehydrogenase. \* =  $P < .05$ , \*\* =  $P < .01$ , and \*\*\* =  $P < .001$ .



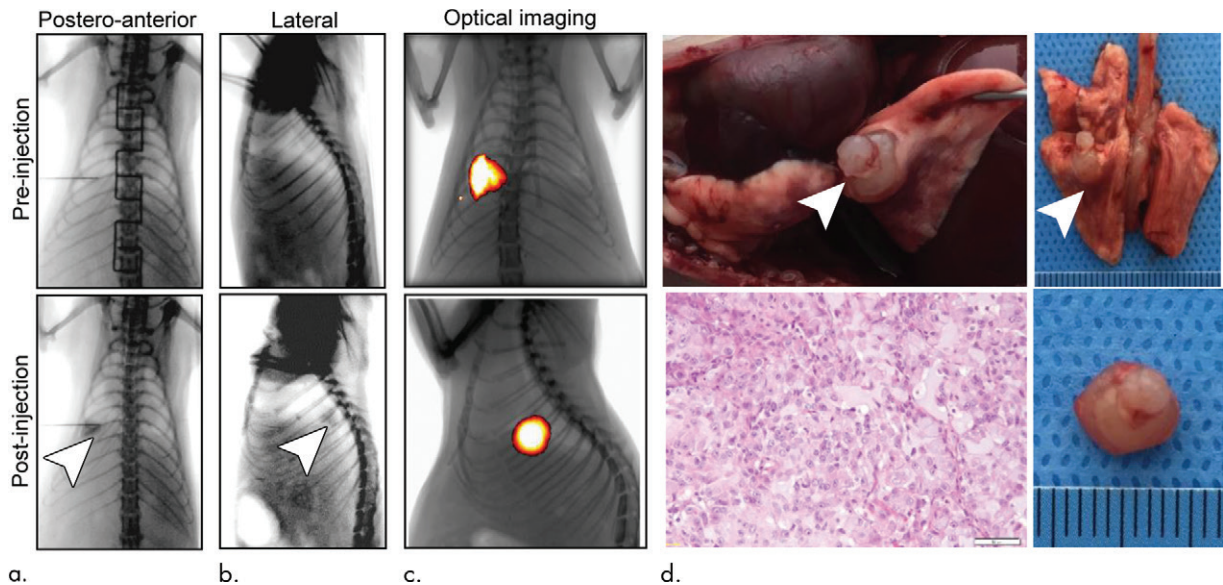


**Figure 5:** Creation of rat model with orthotopic lung cancer. **(a, b)** Under x-ray imaging guidance, a 26-gauge needle was positioned in the lower lobe of the right lung for cell inoculation. Chest radiographs obtained in posteroanterior and lateral projections helped confirm the deposit of injected cell pellet mixed with x-ray contrast agent (arrowheads) in the lung. **(c)** Bioluminescence imaging 3 weeks after cell injection depicted bioluminescence signals emitted from the lung cancer (orange-yellow). **(d)** Gross pathologic and histologic assessments further helped confirm formation of adenocarcinoma within the right lower lobe (original magnification,  $\times 200$ ).

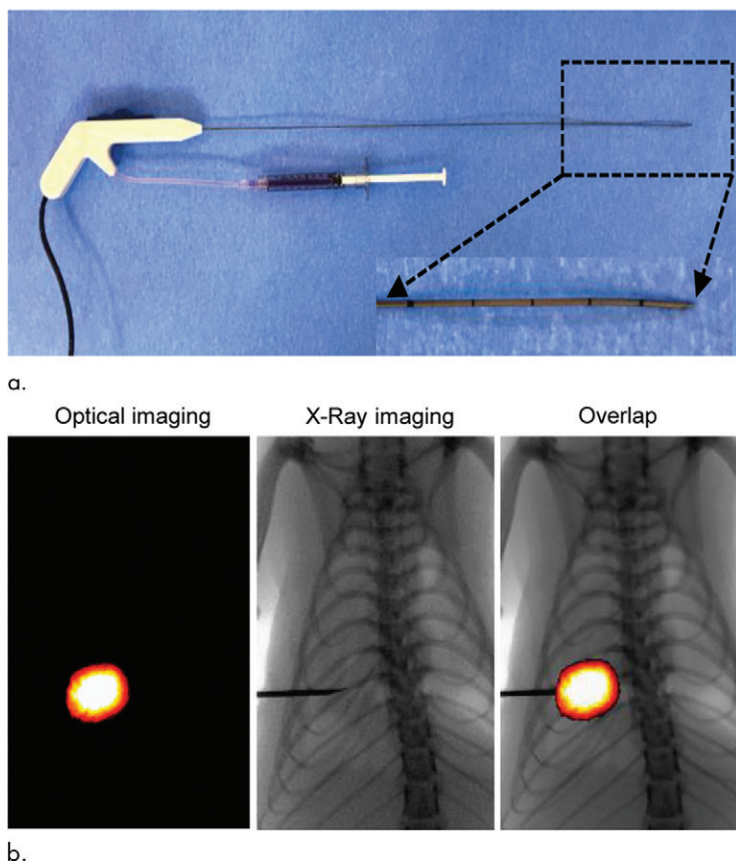


**Figure 6:** X-ray and optical imaging-guided intratumoral gene therapy of rat orthotopic lung cancer. **(a)** Monopolar radiofrequency and perfusion electrode was used to deliver radiofrequency hyperthermia and herpes simplex virus thymidine kinase/lentiviral particles simultaneously into the tumor. **(b)** Under x-ray and optical imaging guidance, the radiofrequency and perfusion electrode was precisely positioned into the lung tumor.

with Ki-67 staining showed suppressed cell proliferation with combination therapy compared with other treatments (mean: 0.11 [95% CI: 0.07, 0.15] vs 0.47 [95% CI: 0.42, 0.51] for RFH, 0.26 [95% CI: 0.20, 0.33] for HSV-TK/GCV, and 0.55 [95% CI: 0.48, 0.61] for phosphate-buffered saline; all  $P < .001$ ). The TUNEL assay demonstrated remarkably increased apoptosis in the combination therapy group (mean: 0.55 [95% CI: 0.31, 0.79] vs 0.02 [95% CI: 0.01, 0.04] for RFH, 0.04 [95% CI: 0.01, 0.07] for HSV-TK/GCV, and 0.001 [95% CI: 0.001, 0.02] for phosphate-buffered saline; all  $P < .05$ ).

## Discussion

Our study has validated the feasibility and efficacy of using RFH to enhance intratumoral HSV-TK/GCV gene therapy for human NSCLC, as evidenced by decreased cell survival in in vitro experiments and decreased tumor volumes and optical signal intensities of both mouse subcutaneous NSCLC xenografts and rat orthotopic lung cancers. Our study also demonstrated that (a) it is feasible to deliver GFP/HSV-TK/lentivirus directly into the NSCLC tumors in the setting of concomitant RFH generation with x-ray and optical imaging guidance and (b) optical imaging is a useful tool with which to assess the response of NSCLC tumors to the RFH-enhanced intratumoral gene therapy.

Numerous preclinical studies on rodent cancer models have confirmed the efficacy of HSV-TK/GCV-mediated gene therapy on tumors (14,18–20). However, most of these treatments were performed via systemic delivery approaches, which are limited by low

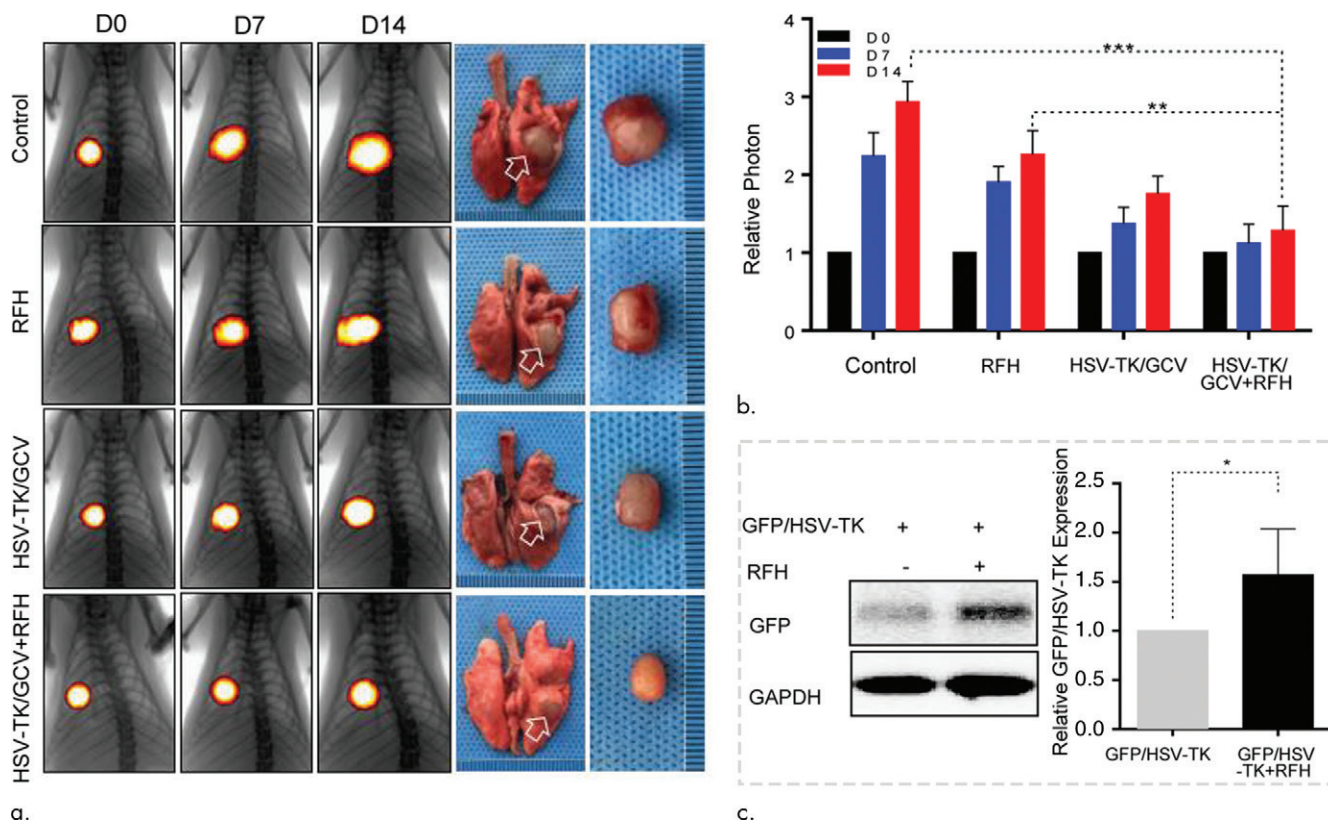


**Figure 7:** In vivo experiments for validating the feasibility of the technique using rat models with orthotopic lung tumors, with four different treatment groups (herpes simplex virus [HSV] thymidine kinase [TK]/ganciclovir [GCV] plus radiofrequency hyperthermia [RFH], RFH alone, HSV-TK/GCV alone, and phosphate-buffered saline). **(a, b)** X-ray and optical imaging showed a smaller increase of mean bioluminescence signals (red-yellow) in the combination therapy group compared with the other three groups (HSV-TK/GCV plus RFH, 1.29 [95% confidence interval {CI}, 0.51, 2.06] vs RFH, 2.26 [95% CI: 1.51, 3.01]; HSV-TK/GCV, 1.76 [95% CI: 1.20, 2.31]; phosphate-buffered saline, 2.94 [95% CI: 2.29, 3.58];  $P < .001$ ). Error bars indicate the standard deviation. Subsequent pathologic evaluation showed that the smallest tumor size occurred in the combination therapy group. **(c)** Western blotting analysis of tumor tissues was used to confirm significantly enhanced green fluorescent protein (GFP) gene expression in tumors treated with RFH compared with tumors without RFH treatment (GFP/HSV-TK plus RFH, 1.57 [95% CI: 1.08, 2.06] vs GFP/HSV-TK, 1.00 [95% CI: 1.00, 1.00];  $P < .05$ ; six animals per group). Error bar indicates the standard deviation. GAPDH = glyceraldehyde 3-phosphate dehydrogenase. \* =  $P < .05$ , \*\* =  $P < .01$ , and \*\*\* =  $P < .001$ .

delivery doses of therapeutic genes to target tumors. Inability to specifically deliver a high dose of therapeutic genes has been a major obstacle in translating the HSV-TK/GCV-mediated suicide gene therapy to wide clinical practice. In our study, we directly injected GFP/HSV-TK/lentiviruses into rat orthotopic lung tumors through the perfusion needle of a multifunctional radiofrequency electrode, thus establishing a method of image-guided local delivery of high-dose therapeutic genes into the target tumor while simultaneously applying thermal energy to enhance the tumoricidal effects. This combinatorial local-regional approach can potentially minimize the toxicity and immunogenicity caused by the systemic administration of exogenous genes, thereby improving the safety profile of gene therapy in patients.

Currently, the most widely used animal models of lung tumors are created in immunodeficient rodents, such as nude and severe combined immunodeficiency mice with subcutaneous lung cancer xenografts. However, these types of lung cancer models cannot exhibit the site-specific pathophysiologic properties of human lung cancers and the interactions between tumors and host organs. We created a molecular imaging-detectable rat model with orthotopic lung tumors via an imaging-guided

percutaneous intrapulmonary approach. We confirmed that this rat model is large enough to accommodate investigation with a clinically used radiofrequency ablation device. In addition, we prelabeled the lung cancer cells with the luciferase gene, which enabled us to use bioluminescence optical imaging to detect the tumor in vivo, guide the targeted interventions, and follow-up treatment responses.

Our study had some limitations. We followed-up the therapeutic effects on animals over only 14 days. This limit was set because tumors in the control group might grow larger than 10% of the host body weight after 14 days, which was not approved by the institutional animal care and use committee. For our proof-of-principle study, we did not compare the treatment efficacies between the intratumoral and systemic administration approaches and the RFH-enhanced HSV-TK/GCV gene therapy.

In conclusion, intratumoral RFH can enhance the HSV-TK/GCV-mediated suicide gene therapy for NSCLC, as guided and monitored with molecular imaging. This method may introduce a way to effectively manage unresectable lung cancer by integrating advances in interventional molecular imaging, radiofrequency technology, and direct intratumoral gene therapy.



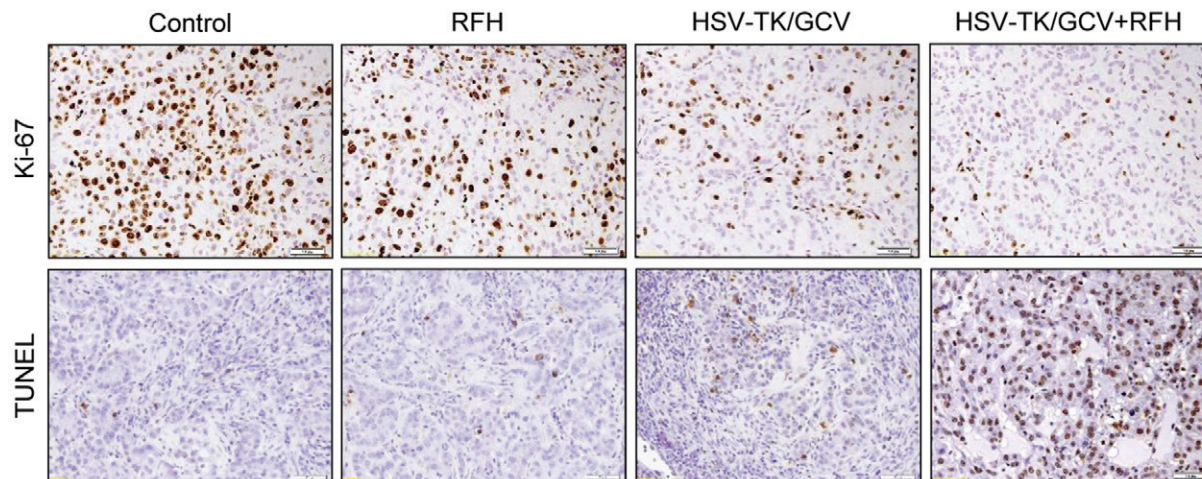


**Figure 8:** Immunohistochemical staining of rat orthotopic tumor tissues after the four different treatments. Ki-67 staining showed substantial inhibition of cancer cell proliferation in the combination therapy group, as evidenced by the fewest brown-stained cells (mean: herpes simplex virus [HSV] thymidine kinase [TK]/ganciclovir [GCV] plus radiofrequency hyperthermia [RFH], 0.11 [95% confidence interval (CI): 0.07, 0.15] vs RFH, 0.47 [95% CI: 0.42, 0.51]; HSV-TK/GCV, 0.26 [95% CI: 0.20, 0.33]; and phosphate-buffered saline, 0.55 [95% CI: 0.48, 0.61]; all  $P < .001$ ). Terminal deoxynucleotidyl transferase-mediated 29-deoxyuridine, 59-triphosphate nick end labeling staining for apoptosis demonstrated an enhanced tumoricidal effect of combination therapy, as evidenced by the largest number of brown-stained cells in this treatment group (original magnification,  $\times 200$ ) (mean: HSV-TK/GCV plus RFH, 0.55 [95% CI: 0.31, 0.79] vs RFH, 0.02 [95% CI: 0.01, 0.04]; HSV-TK/GCV, 0.04 [95% CI: 0.01, 0.07]; and phosphate-buffered saline, 0.001 [95% CI: 0.001, 0.02];  $P < .05$ ). *TUNEL* = terminal deoxynucleotidyl transferase-mediated 2'-deoxyuridine, 5'-triphosphate nick end labeling.

**Author contributions:** Guarantors of integrity of entire study, J.J., F.Z., F.X., M.C., X.Y.; study concepts/study design or data acquisition or data analysis/interpretation, all authors; manuscript drafting or manuscript revision for important intellectual content, all authors; approval of final version of submitted manuscript, all authors; agrees to ensure any questions related to the work are appropriately resolved, all authors; literature research, J.J., Y.J., M.C., Q.L.; experimental studies, J.J., Q.W., F.Z., F.X., Y.J., J.H., J.S., J.G., M.C., X.Y.; statistical analysis, F.X., Y.J., M.C.; and manuscript editing, J.J., Y.J., M.C.

**Disclosures of Conflicts of Interest:** J.J. disclosed no relevant relationships. Q.W. disclosed no relevant relationships. F.Z. disclosed no relevant relationships. F.X. disclosed no relevant relationships. Y.J. disclosed no relevant relationships. J.H. disclosed no relevant relationships. J.S. disclosed no relevant relationships. J.G. disclosed no relevant relationships. M.C. disclosed no relevant relationships. Q.L. disclosed no relevant relationships. D.S. disclosed no relevant relationships. X.Y. disclosed no relevant relationships.

## References

- Reck M, Popat S, Reinmuth N, et al. Metastatic non-small-cell lung cancer (NSCLC): ESMO Clinical Practice Guidelines for diagnosis, treatment and follow-up. *Ann Oncol* 2014;25(Suppl 3):iii27–iii39.
- Chang JY, Senan S, Paul MA, et al. Stereotactic ablative radiotherapy versus lobectomy for operable stage I non-small-cell lung cancer: a pooled analysis of two randomised trials. *Lancet Oncol* 2015;16(6):630–637.
- Veeramachaneni NK, Feins RH, Stephenson BJ, Edwards LJ, Fernandez FG. Management of stage IIIA non-small cell lung cancer by thoracic surgeons in North America. *Ann Thorac Surg* 2012;94(3):922–926; discussion 926–928.
- Ambrogi MC, Fanucchi O, Cioni R, et al. Long-term results of radiofrequency ablation treatment of stage I non-small cell lung cancer: a prospective intention-to-treat study. *J Thorac Oncol* 2011;6(12):2044–2051.
- Healey TT, March BT, Baird G, Dupuy DE. Microwave ablation for lung neoplasms: a retrospective analysis of long-term results. *J Vasc Interv Radiol* 2017;28(2):206–211.
- Kodama H, Yamakado K, Hasegawa T, et al. Radiofrequency ablation using a multiple-electrode switching system for lung tumors with 2.0–5.0-cm maximum diameter: phase II clinical study. *Radiology* 2015;277(3):895–902.
- Kodama H, Yamakado K, Hasegawa T, et al. Radiofrequency ablation for ground-glass opacity-dominant lung adenocarcinoma. *J Vasc Interv Radiol* 2014;25(3):333–339.
- Planché O, Teritehau C, Boudabous S, et al. In vivo evaluation of lung microwave ablation in a porcine tumor mimic model. *Cardiovasc Intervent Radiol* 2013;36(1):221–228.
- Sato T, Yanagisawa T. The engineered thymidylate kinase (TMPK)/azidothymidine (AZT)-axis offers efficient bystander cell killing effect for suicide gene therapy for cancer [in Japanese]. *Nippon Yakurigaku Zasshi* 2016;147(6):326–329.
- Sangro B, Mazzolini G, Ruiz M, et al. A phase I clinical trial of thymidine kinase-based gene therapy in advanced hepatocellular carcinoma. *Cancer Gene Ther* 2010;17(12):837–843.
- Hung CF, Chiang AJ, Tsai HH, et al. Ovarian cancer gene therapy using HPV-16 pseudovirion carrying the HSV-tk gene. *PLoS One* 2012;7(7):e40983.
- Zhang JF, Wei F, Wang HP, et al. Potent anti-tumor activity of telomerase-dependent and HSV-TK armed oncolytic adenovirus for non-small cell lung cancer in vitro and in vivo. *J Exp Clin Cancer Res* 2010;29(1):52.
- Kurdow R, Schniewind B, Boehle AS, et al. Resistance developing after long-term ganciclovir prodrug treatment in a preclinical model of NSCLC. *Anticancer Res* 2004;24(2B):827–831.
- Shi Y, Wang J, Bai Z, et al. Radiofrequency hyperthermia-enhanced herpes simplex virus-thymidine kinase/ganciclovir direct intratumoral gene therapy of esophageal squamous cancers. *Am J Cancer Res* 2016;6(9):2054–2063.
- Zhang F, Le T, Wu X, et al. Intrabiliary RF heat-enhanced local chemotherapy of a cholangiocarcinoma cell line: monitoring with dual-modality imaging—preclinical study. *Radiology* 2014;270(2):400–408.
- Zhang F, Li J, Meng Y, et al. Development of an intrabiliary MR imaging-monitored local agent delivery technique: a feasibility study in pigs. *Radiology* 2012;262(3):846–852.
- Shi Z, Cai Z, Sanchez A, et al. A novel Toll-like receptor that recognizes vesicular stomatitis virus. *J Biol Chem* 2011;286(6):4517–4524.
- Leinonen HM, Ruotsalainen AK, Määttä AM, et al. Oxidative stress-regulated lentiviral TK/GCV gene therapy for lung cancer treatment. *Cancer Res* 2012;72(23):6227–6235.
- Singh S, Cunningham C, Buchanan A, Jolly DJ, Nemunaitis J. Toxicity assessment of intratumoral injection of the herpes simplex type I thymidine kinase gene delivered by retrovirus in patients with refractory cancer. *Mol Ther* 2001;4(2):157–160.
- Zarogoulidis P, Chatzaki E, Hohenforst-Schmidt W, et al. Management of malignant pleural effusion by suicide gene therapy in advanced stage lung cancer: a case series and literature review. *Cancer Gene Ther* 2012;19(9):593–600.